ON INTERPOLATION BY PLANAR CUBIC G^2 PYTHAGOREAN-HODOGRAPH SPLINE CURVES

GAŠPER JAKLIČ, JERNEJ KOZAK, MARJETA KRAJNC, VITO VITRIH,
AND EMIL ŽAGAR

ABSTRACT. In this paper, the geometric interpolation of planar data points and boundary tangent directions by a cubic G^2 Pythagorean-hodograph (PH) spline curve is studied. It is shown, that such an interpolant exists under some natural assumptions on the data. The construction of the spline is based upon the solution of a tridiagonal system of nonlinear equations. The asymptotic approximation order 4 is confirmed.

1. INTRODUCTION

Pythagorean-hodograph (PH) curves ([5, 4]) form a special subclass of planar polynomial parametric curves. They are distinguished by having an exact representation of an arc-length and a rational offset. This makes them very useful in practical applications, such as CAGD, CAD/CAM systems, robotics, animation,... Although they have less degrees of freedom than general parametric curves, they still admit nice shape properties, which makes them interesting in shape preserving techniques. The parametric and the geometric Hermite interpolation are nowadays well established approaches for an approximation of discrete data by polynomial parametric objects. In the last decade a lot of results on a Hermite type interpolation have been obtained (see [7], [1], [13], [11], [15], [6], [14], e.g.). It is well-known that regular PH curves must be of odd degrees. This clearly reduces spline interpolants to the cubic and the quintic case, perhaps even up to degree seven. Higher degrees are rarely used since PH characterization equations become too complicated.

In [13], a G^1 continuous Hermite interpolation by PH cubics was considered. The interpolating cubic PH curve is determined by the local data only and the construction is based upon data points and tangent directions at these points. However, tangent directions are often hard to obtain. So why not to look for a cubic PH interpolant based upon data points only (except at the boundary) as it is shown in Fig. 1. But at the same time the approximation order achieved should stay optimal and the obtained interpolant should preserve some shape properties of the data (convexity e.g., formally defined in (2.2)).

This suggests a natural interpolation problem to be considered, i.e., an interpolation of planar data points and tangent directions at the boundary by a cubic G^2 PH spline. This kind of problem was somehow overlooked in the past. One of
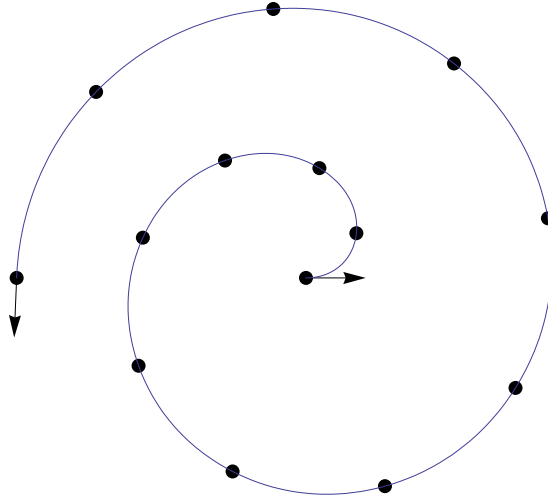
FIGURE 1. A cubic G^2 PH curve.

the reasons might have been the fact that cubic PH curves are restricted to basically only one curve (up to translation, rotation, scaling and reparameterization), namely the Tschirnhausen's cubic [8]. As it is well known it has no inflection points, which restricts the interpolation flexibility. Nevertheless, a cubic interpolatory G^2 PH spline is a simple tool that preserves convexity of the data. Also, it offers the arc-length reparameterization of the spline curve in a closed form. On the other hand, since a cubic PH curve is without inflection points, a cubic G^2 PH spline must possess the same property. Thus this scheme is not appropriate for interpolation of free-form data in its basic form. To overcome this obstacle, a simple preprocessing algorithm is suggested that breaks down the general data to convex segments.

In this paper, an interpolation of convex planar data points and tangent directions at the boundary by a cubic G^2 PH spline is considered. Under some natural assumptions on the data, the existence of the interpolating cubic G^2 PH spline is shown and the approximation order 4 is confirmed. As a special case and a basis for the induction step, the cubic Hermite PH interpolation is studied in detail, and the results in [12] are enhanced. The obtained results naturally extend to the closed curve interpolation.

If the data points fail to be convex, a preprocessing algorithm for point insertion is proposed in the last section of the paper. In this case a tangent direction at a new breakpoint is prescribed which reduces the G^2 to G^1 continuity at that point.

The outline of the paper is as follows. In Section 2 the interpolation problem considered is presented, and the main results of the paper are given. In the next section the single segment, a cornerstone of a PH cubic spline interpolation, is analysed. In Section 4, a proof of the main result is outlined, and in the next section an asymptotic approximation order is studied. The paper is concluded by some numerical examples and a preprocessing algorithm for point insertion.

2. INTERPOLATION PROBLEM

Let us introduce the interpolation problem considered. Suppose that data

$$(2.1) \qquad \boldsymbol{d}_0, \boldsymbol{P}_0, \boldsymbol{P}_1, \ldots, \boldsymbol{P}_m, \boldsymbol{d}_m, \quad \boldsymbol{P}_\ell \neq \boldsymbol{P}_{\ell+1},$$

are prescribed, where $\boldsymbol{P}_\ell$ denotes a point in $\mathbb{R}^2$ to be interpolated, and $\boldsymbol{d}_\ell$, $\|\boldsymbol{d}_\ell\| = 1$, is the tangent direction at the boundary point $\boldsymbol{P}_\ell$, $\ell = 0, m$. Our goal is to construct an interpolating G^2 cubic PH spline curve $\boldsymbol{B}$. In order to overcome the problem of inflections, we will assume throughout the paper, that the data (2.1) are *convex*. In the last section of the paper, this restriction will be surmounted by a preprocessing algorithm for dealing with general data. In this case the resulting spline curve will not be globally G^2 but nonetheless it will be loop-free.

Before we introduce convexity, some additional notation is needed. The norm $\|\cdot\|$ will denote the Euclidean norm, implied by the scalar product $\boldsymbol{u} \cdot \boldsymbol{v}$, and $\boldsymbol{u} \times \boldsymbol{v}$ will be the planar vector product. Furthermore, $\angle(\boldsymbol{u}, \boldsymbol{v})$ will be the angle between vectors $\boldsymbol{u}$ and $\boldsymbol{v}$, and $\Delta \boldsymbol{P}_\ell := \boldsymbol{P}_{\ell+1} - \boldsymbol{P}_\ell$. The term *convex* refers to the requirement that $\Delta \boldsymbol{P}_\ell \times \Delta \boldsymbol{P}_{\ell+1}$ is of the same sign for any two consecutive $\Delta \boldsymbol{P}_\ell$, $\ell = 0, 1, \ldots, m-1$, and for the appropriate vector products at the boundary. Without loss of generality, we may assume throughout the paper that this sign is positive, i.e.,

$$(2.2) \qquad \begin{aligned} \boldsymbol{d}_0 \times \Delta \boldsymbol{P}_0 &> 0, \\ \Delta \boldsymbol{P}_\ell \times \Delta \boldsymbol{P}_{\ell+1} &> 0, \quad \ell = 0, 1, \ldots, m-2, \\ \Delta \boldsymbol{P}_{m-1} \times \boldsymbol{d}_m &> 0. \end{aligned}$$

Now let us consider the smoothness and PH conditions of the G^2 cubic PH interpolating spline $\boldsymbol{B}$. A natural approach is to express segments $\boldsymbol{B}^\ell$ of the spline curve $\boldsymbol{B}$ as cubic Bézier curves

$$(2.3) \qquad \boldsymbol{B}^\ell := \sum_{i=0}^{3} \boldsymbol{b}_{3\ell-3+i} B_{3,i}.$$

Here, $B_{n,i}$ are the cubic Bernstein basis polynomials of degree n, and

$$\boldsymbol{b}_i \in \mathbb{R}^2, \quad i = 0, 1, \ldots, 3m,$$

are the control points of the spline curve that satisfy the end-point interpolation property of Bézier curves, i.e.,

$$\boldsymbol{b}_{3\ell} = \boldsymbol{P}_\ell, \quad \ell = 0, 1, \ldots, m.$$

The remaining $4m$ unknowns $\boldsymbol{b}_{3\ell-2}$, $\boldsymbol{b}_{3\ell-1}$, $\ell = 1, 2, \ldots, m$, need to be determined by the fact that the interpolating curve is G^2 continuous and piecewise PH.

As can be seen in Fig. 3, not every PH interpolatory cubic spline preserves the shape of the data (2.2). Although it is a convex curve it can have undesired loops (see [12, 10], e.g.). In order to avoid this, we will require that the control polygon of every spline segment satisfies

$$\Delta \boldsymbol{b}_{3\ell-3} \times \Delta \boldsymbol{b}_{3\ell-2} > 0, \quad \Delta \boldsymbol{b}_{3\ell-2} \times \Delta \boldsymbol{b}_{3\ell-1} > 0, \quad \ell = 1, 2, \ldots, m.$$

Such an interpolatory cubic spline curve will be called *admissible*.

The G^1 continuity requires collinearity of the tangents at $\boldsymbol{P}_\ell$ [9, e.g.], i.e.,

$$(2.4) \qquad \begin{aligned} \boldsymbol{d}_0 \times \Delta \boldsymbol{b}_0 &= 0, \\ \Delta \boldsymbol{b}_{3\ell-1} \times \Delta \boldsymbol{b}_{3\ell} &= 0, \quad \ell = 1, 2, \ldots, m-1, \\ \Delta \boldsymbol{b}_{3m-1} \times \boldsymbol{d}_m &= 0, \end{aligned}$$

and the curvature continuity conditions at $\boldsymbol{P}_\ell$, $\ell = 1, 2, \ldots, m-1$, are

$$(2.5) \qquad \frac{\Delta\boldsymbol{b}_{3\ell-1} \times (-\Delta\boldsymbol{P}_{\ell-1} + \Delta\boldsymbol{b}_{3\ell-3})}{\|\Delta\boldsymbol{b}_{3\ell-1}\|^3} = \frac{\Delta\boldsymbol{b}_{3\ell} \times (\Delta\boldsymbol{P}_\ell - \Delta\boldsymbol{b}_{3\ell+2})}{\|\Delta\boldsymbol{b}_{3\ell}\|^3}.$$

Note that the closed curve interpolation problem can be stated in a similar way thus its analysis will be omitted.

By (2.4) the directions of $\Delta\boldsymbol{b}_{3\ell-1}$ and $\Delta\boldsymbol{b}_{3\ell}$ should agree. Thus it is natural to introduce

$$\boldsymbol{d}_\ell, \quad \|\boldsymbol{d}_\ell\| = 1, \quad \ell = 1, 2, \ldots, m-1,$$

as unknown tangent directions at $\boldsymbol{P}_\ell$. Recall that $\boldsymbol{d}_0$ and $\boldsymbol{d}_m$ are prescribed. The unknown differences of control points can be expressed as

$$(2.6) \qquad \Delta\boldsymbol{b}_{3\ell} = \lambda_{2\ell}\boldsymbol{d}_\ell, \quad \Delta\boldsymbol{b}_{3\ell+2} = \lambda_{2\ell+1}\boldsymbol{d}_{\ell+1}, \quad \ell = 0, 1, \ldots, m-1.$$

Provided the tangent directions $\boldsymbol{d}_\ell$ and $\boldsymbol{d}_{\ell+1}$ are known, the lengths $\lambda_{2\ell} = \|\Delta\boldsymbol{b}_{3\ell}\|$ and $\lambda_{2\ell+1} = \|\Delta\boldsymbol{b}_{3\ell+2}\|$ are determined from a PH characterization (see [12]). Thus, $\lambda_{2\ell} = \lambda_{2\ell}(\boldsymbol{d}_\ell, \boldsymbol{d}_{\ell+1})$, $\lambda_{2\ell+1} = \lambda_{2\ell+1}(\boldsymbol{d}_\ell, \boldsymbol{d}_{\ell+1})$, and with the help of (2.6) the curvature continuity conditions (2.5) simplify to $m-1$ equations

$$\boldsymbol{d}_\ell \times \left(\frac{1}{\lambda_{2\ell}^2} (\Delta\boldsymbol{P}_\ell - \lambda_{2\ell+1}\boldsymbol{d}_{\ell+1}) + \frac{1}{\lambda_{2\ell-1}^2} (\Delta\boldsymbol{P}_{\ell-1} - \lambda_{2\ell-2}\boldsymbol{d}_{\ell-1}) \right) = 0,$$

$$(2.7) \qquad\qquad\qquad\qquad\qquad\qquad\qquad\qquad \ell = 1, 2, \ldots, m-1,$$

for $m-1$ unknown directions $\boldsymbol{d}_\ell$. The main results of the paper can now be stated as follows.

Theorem 2.1. *Suppose that the data (2.1) are convex as explained in (2.2). The system of nonlinear equations (2.7) has an admissible solution if and only if the angles*

$$\varphi_0 := \angle(\boldsymbol{d}_0, \Delta\boldsymbol{P}_0),$$
$$\varphi_\ell := \angle(\Delta\boldsymbol{P}_{\ell-1}, \Delta\boldsymbol{P}_\ell), \quad \ell = 1, 2, \ldots, m-1,$$
$$\varphi_m := \angle(\Delta\boldsymbol{P}_{m-1}, \boldsymbol{d}_m),$$

satisfy $\varphi_i + \varphi_{i+1} < 4\pi/3$ for $i = 0, 1, \ldots, m-1$. If the upper bound is decreased to $K\pi$,

$$K := 1 + \frac{1}{\pi}\arccos\left(\frac{\sqrt{3}}{3}\right) \approx 1.304087 < 4/3,$$

the solution is unique.

Theorem 2.2. *The asymptotic approximation order of the solution, obtained by the assertions of Theorem 2.1, is 4.*

3. SINGLE SEGMENT

In order to prove Theorem 2.1, we have to consider the single segment case first. So let us assume $m = 1$ through the rest of this section. The cubic Hermite PH interpolation has already been analysed in [12], but here some additional facts will be outlined. In particular, not all tangent directions that form convex data give admissible solutions, a fact that was overlooked in [12]. As stated in Theorem 2.1, an additional angle restriction is necessary in order for the solution to exist. Furthermore, besides the unique admissible solution, a solution with a loop may exist. Explicit formulae for both solutions will be given.
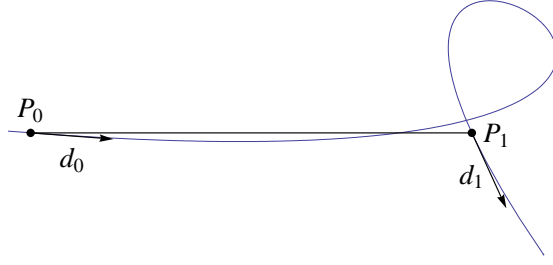
FIGURE 2. Inappropriate data which lead to a cubic PH interpolant with a loop.

For a single segment, the prescribed data are

$$\boldsymbol{d}_0,\ \boldsymbol{P}_0,\ \boldsymbol{P}_1,\ \boldsymbol{d}_1,$$

and the convexity requirements become

$$(3.1) \qquad \boldsymbol{d}_0 \times \Delta\boldsymbol{P}_0 > 0, \quad \Delta\boldsymbol{P}_0 \times \boldsymbol{d}_1 > 0.$$

Note that a solution may still exist if the suppositions (3.1) are violated, but it usually has a loop since no inflection points are possible (see Fig. 2). This is undesirable for a shape preserving spline interpolation.

The cubic interpolatory Bézier curve $\boldsymbol{B}$ is determined by control points $\boldsymbol{b}_i$,

$$(3.2) \qquad \boldsymbol{b}_0 = \boldsymbol{P}_0, \quad \boldsymbol{b}_1 = \boldsymbol{P}_0 + \lambda_0\boldsymbol{d}_0, \quad \boldsymbol{b}_2 = \boldsymbol{P}_1 - \lambda_1\boldsymbol{d}_1, \quad \boldsymbol{b}_3 = \boldsymbol{P}_1.$$

Our goal is to obtain the parameters $\lambda_i > 0$, $i = 0, 1$. A well known characterization of cubic PH curves in Bézier form [8] will be used. First, the equality of angles ([8])

$$\angle\left(\Delta\boldsymbol{b}_0, \Delta\boldsymbol{b}_1\right) = \angle\left(\Delta\boldsymbol{b}_1, \Delta\boldsymbol{b}_2\right),$$

can be by (3.1) simplified to

$$\cos\left(\angle\left(\Delta\boldsymbol{b}_0, \Delta\boldsymbol{b}_1\right)\right) = \cos\left(\angle\left(\Delta\boldsymbol{b}_1, \Delta\boldsymbol{b}_2\right)\right),$$

or equivalently

$$(3.3) \qquad \left(\boldsymbol{d}_0 - \boldsymbol{d}_1\right)\cdot\Delta\boldsymbol{b}_1 = 0.$$

Thus, with new unknowns ξ_i, introduced as

$$(3.4) \qquad \xi_0 := \frac{\lambda_0 - \lambda_1}{2\|\Delta\boldsymbol{P}_0\|}, \quad \xi_1 := \frac{\lambda_0 + \lambda_1}{2\|\Delta\boldsymbol{P}_0\|},$$

and

$$\boldsymbol{v} := \frac{1}{\|\Delta\boldsymbol{P}_0\|}\,\Delta\boldsymbol{P}_0,$$

the equation (3.3) simplifies to

$$(3.5) \qquad \xi_0 = \Xi_0\left(\boldsymbol{d}_0, \boldsymbol{v}, \boldsymbol{d}_1\right) := \frac{1}{2}\frac{\left(\boldsymbol{d}_0 - \boldsymbol{d}_1\right)\cdot\boldsymbol{v}}{1 - \boldsymbol{d}_0\cdot\boldsymbol{d}_1}.$$

The second characteristic equation of cubic PH curves ([8]) is

$$\|\Delta\boldsymbol{b}_1\| = \sqrt{\|\Delta\boldsymbol{b}_0\|\,\|\Delta\boldsymbol{b}_2\|}.$$

By (3.2), (3.4) and (3.5) it can be written as a quadratic equation for ξ_1,

$$(3.6) \qquad \left(1 + 2\, \boldsymbol{d}_0 \cdot \boldsymbol{d}_1\right) \xi_1^2 - 2\left(\boldsymbol{d}_0 + \boldsymbol{d}_1\right) \cdot \boldsymbol{v}\, \xi_1 + 1 - \left(1 - 2\, \boldsymbol{d}_0 \cdot \boldsymbol{d}_1\right) \xi_0^2 = 0.$$

Its solutions are

$$(3.7) \quad \xi_1^{\pm} = \Xi_1^{\pm}\left(\boldsymbol{d}_0, \boldsymbol{v}, \boldsymbol{d}_1\right) :=$$

$$= \frac{1 - (1 - 2\boldsymbol{d}_0 \cdot \boldsymbol{d}_1)\xi_0^2}{(\boldsymbol{d}_0 + \boldsymbol{d}_1) \cdot \boldsymbol{v} \pm \sqrt{((\boldsymbol{d}_0 + \boldsymbol{d}_1) \cdot \boldsymbol{v})^2 - (1 - (1 - 2\boldsymbol{d}_0 \cdot \boldsymbol{d}_1)\xi_0^2)(1 + 2\, \boldsymbol{d}_0 \cdot \boldsymbol{d}_1)}},$$

where ξ_0 satisfies (3.5). From (3.4), (3.5), and (3.7) we obtain solutions of the interpolation problem

$$\lambda_0^{\pm} = \Lambda_0^{\pm}\left(\boldsymbol{d}_0, \Delta \boldsymbol{P}_0, \boldsymbol{d}_1\right) :=$$

$$(3.8) \qquad := \|\Delta \boldsymbol{P}_0\| \left(\Xi_1^{\pm}\left(\boldsymbol{d}_0, \frac{\Delta \boldsymbol{P}_0}{\|\Delta \boldsymbol{P}_0\|}, \boldsymbol{d}_1\right) + \Xi_0\left(\boldsymbol{d}_0, \frac{\Delta \boldsymbol{P}_0}{\|\Delta \boldsymbol{P}_0\|}, \boldsymbol{d}_1\right) \right),$$

$$\lambda_1^{\pm} = \Lambda_1^{\pm}\left(\boldsymbol{d}_0, \Delta \boldsymbol{P}_0, \boldsymbol{d}_1\right) :=$$

$$:= \|\Delta \boldsymbol{P}_0\| \left(\Xi_1^{\pm}\left(\boldsymbol{d}_0, \frac{\Delta \boldsymbol{P}_0}{\|\Delta \boldsymbol{P}_0\|}, \boldsymbol{d}_1\right) - \Xi_0\left(\boldsymbol{d}_0, \frac{\Delta \boldsymbol{P}_0}{\|\Delta \boldsymbol{P}_0\|}, \boldsymbol{d}_1\right) \right),$$

and (3.2) yields the control points $\boldsymbol{b}_i$ of the interpolant $\boldsymbol{B}$.

Note that a translation or a rotation of the coordinate system does not change the values of ξ_0 in (3.5), and $\xi_1^{\pm}$ in (3.7). Thus let us assume from now on till the end of this section that $\boldsymbol{P}_0$ and $\boldsymbol{P}_1$ lie on the x-axis, and that the tangent directions are given by the angles $\varphi_0 = \angle\left(\boldsymbol{d}_0, \Delta \boldsymbol{P}_0\right)$ and $\varphi_1 = \angle\left(\Delta \boldsymbol{P}_0, \boldsymbol{d}_1\right)$. Further discussion will be simplified by introducing new parameters β_0 and β_1, satisfying $\varphi_0 = \beta_1 - \beta_0$, $\varphi_1 = \beta_1 + \beta_0$. Now,

$$(3.9) \qquad \boldsymbol{d}_0 = \begin{bmatrix} \cos(\beta_1 - \beta_0) \\ -\sin(\beta_1 - \beta_0) \end{bmatrix}, \quad \boldsymbol{v} = \begin{bmatrix} 1 \\ 0 \end{bmatrix}, \quad \boldsymbol{d}_1 = \begin{bmatrix} \cos(\beta_1 + \beta_0) \\ \sin(\beta_1 + \beta_0) \end{bmatrix}.$$

To fulfill the convexity requirements (3.1), the angles β_i are restricted to

$$(3.10) \qquad I := \{(\beta_0, \beta_1) : 0 < \beta_1 \leq \pi, \ |\beta_0| < \min\{\beta_1, \pi - \beta_1\}\}.$$

The assumption (3.9) simplifies ξ_0 in (3.5) to

$$(3.11) \qquad\qquad\qquad \xi_0 = \frac{1}{2} \frac{\sin \beta_0}{\sin \beta_1},$$

and $\xi_1^{\pm}$ in (3.7) to

$$(3.12) \qquad\qquad\qquad \xi_1^{\pm} = \frac{A_1(\beta_0, \beta_1)}{A_2(\beta_0, \beta_1) \pm \sqrt{A_3(\beta_0, \beta_1)}},$$

where

$$A_1(\beta_0, \beta_1) := \cos^2 \beta_0 + \frac{1}{4} \frac{\sin^2 \beta_0}{\sin^2 \beta_1}, \quad A_3(\beta_0, \beta_1) := 1 - \frac{3}{4} \frac{\sin^2 \beta_0}{\sin^2 \beta_1},$$

and $A_2(\beta_0, \beta_1) := 2 \cos \beta_0 \cos \beta_1$. It is clear that $-\frac{1}{2} < \xi_0 < \frac{1}{2}$. Since λ_i must be positive, this must be also true for $\xi_1^{\pm}$.

Lemma 3.1. *Let $\xi_1^{\pm}$ be given by (3.12). Then ξ_1^+ is positive iff*

$$(\beta_0, \beta_1) \in I_+ := \left\{ (\beta_0, \beta_1) \in I, \quad 0 < \beta_1 < \frac{2\pi}{3} \right\},$$

and ξ_1^- is positive iff

$$(\beta_0, \beta_1) \in I_- := \left\{ (\beta_0, \beta_1) \in I, \quad 0 < \beta_1 < \frac{\pi}{3} \right\}.$$

Proof. Since $A_3(\beta_0, \beta_1) > 1/4$, $\xi_1^\pm$ is real. The numerator in (3.12) is clearly positive, but the denominator may vanish. It is straightforward to verify that this happens only if $\beta_1 = \pi/3$ or $\beta_1 = 2\pi/3$. Since $\cos \beta_0 \cos \beta_1 \geq 0$ for $0 < \beta_1 \leq \frac{\pi}{2}$ and $\cos \beta_0 \cos \beta_1 < 0$ for $\frac{\pi}{2} < \beta_1 < \pi$, the denominator in ξ_1^+ is zero iff $\beta_1 = \frac{2}{3}\pi$, and the denominator in ξ_1^- is zero iff $\beta_1 = \frac{1}{3}\pi$. Since

$$\left(A_2(\beta_0, \beta_1) \pm \sqrt{A_3(\beta_0, \beta_1)} \right) \big|_{\beta_0 = 0} = 2 \cos \beta_1 \pm 1 > 0$$

for $(\beta_0, \beta_1) \in I_\pm$, the assertion follows. $\qquad\square$

Lemma 3.2. *Suppose that $(\beta_0, \beta_1) \in I_\pm$. Then $\lambda_i^\pm > 0$, $i = 0, 1$.*

Proof. Note that ξ_0 defined by (3.11) and $\xi_1^\pm$ defined by (3.12) are continuous functions of β_i. Further, by (3.8), $\lambda_0^\pm = 0$ or $\lambda_1^\pm = 0$ iff $\xi_1^\pm = \pm \xi_0$. But, by using (3.11), the equation (3.6) for $\xi_1^\pm = \pm \xi_0$ simplifies to

$$\frac{\sin^2 (\beta_0 \mp \beta_1)}{\sin^2 \beta_1} = 0,$$

which clearly does not have any solution in the domain $I_\pm$. Since for $(0, \beta_1) \in I_\pm$,

$$\lambda_0^\pm = \lambda_1^\pm = \frac{\|\Delta \boldsymbol{P}_0\|}{2 \cos \beta_1 \pm 1} > 0,$$

$\lambda_i^\pm > 0$, $i = 0, 1$, for all $(\beta_0, \beta_1) \in I_\pm$. $\qquad\square$

Now it remains to see whether the solution of the interpolation problem is admissible as far as the shape preservation is concerned. It is enough to consider the sign of the planar vector product $\Delta \boldsymbol{b}_0 \times \Delta \boldsymbol{b}_1$ only. A simple calculation shows

$$(\Delta \boldsymbol{b}_0 \times \Delta \boldsymbol{b}_1)^\pm := \lambda_0^\pm (\boldsymbol{d}_0 \times \Delta \boldsymbol{P}_0 - \lambda_1^\pm \boldsymbol{d}_0 \times \boldsymbol{d}_1) =$$

$$= \pm \|\Delta \boldsymbol{P}_0\| \, \lambda_0^\pm \, \xi_1^\pm \, \cos \beta_0 \, \sin \beta_1 \, \frac{A_4(\beta_0, \beta_1) + 2\sqrt{A_3(\beta_0, \beta_1)}}{2 \, A_1(\beta_0, \beta_1)},$$

where $A_4(\beta_0, \beta_1) := \mp \dfrac{\cos \beta_1}{\cos \beta_0} \dfrac{\sin^2 \beta_0}{\sin^2 \beta_1}$. It is straightforward to verify that $(\Delta \boldsymbol{b}_0 \times \Delta \boldsymbol{b}_1)^+ > 0$ for all $(\beta_0, \beta_1) \in I_+$, and $(\Delta \boldsymbol{b}_0 \times \Delta \boldsymbol{b}_1)^- < 0$ for all $(\beta_0, \beta_1) \in I_-$. Thus the first curve is admissible, but the second one has a loop.

This discussion proves a variation of the theorem found in [12], and adds the angle range considerations that have been there omitted.

Theorem 3.3. *Suppose that $\boldsymbol{d}_0, \boldsymbol{P}_0, \boldsymbol{P}_1, \boldsymbol{d}_1$, $\boldsymbol{P}_0 \neq \boldsymbol{P}_1$, are given convex data and*

$$\varphi_0 = \angle (\boldsymbol{d}_0, \Delta \boldsymbol{P}_0), \quad \varphi_1 = \angle (\Delta \boldsymbol{P}_0, \boldsymbol{d}_1).$$

A unique admissible Hermite interpolating PH cubic curve exists iff the angles φ_i satisfy

$$(3.13) \qquad\qquad \varphi_0 + \varphi_1 < \frac{4}{3}\pi.$$

The interpolating curve in the Bézier form is determined by

$$(3.14) \qquad \lambda_0 = \Lambda_0^+ (\boldsymbol{d}_0, \Delta \boldsymbol{P}_0, \boldsymbol{d}_1), \quad \lambda_1 = \Lambda_1^+ (\boldsymbol{d}_0, \Delta \boldsymbol{P}_0, \boldsymbol{d}_1),$$

with Λ_i^+ given by (3.8).

Remark 3.4. Suppose that the suppositions of Theorem 3.3 hold true. If $\varphi_0 + \varphi_1 < \frac{2}{3}\pi$, then besides (3.14) there exists an another Hermite interpolating PH cubic curve, determined by

$$\lambda_0 = \Lambda_0^- \left(\boldsymbol{d}_0, \Delta \boldsymbol{P}_0, \boldsymbol{d}_1\right), \quad \lambda_1 = \Lambda_1^- \left(\boldsymbol{d}_0, \Delta \boldsymbol{P}_0, \boldsymbol{d}_1\right),$$

with Λ_i^- given by (3.8). This solution is not shape preserving, since it has a loop (see Fig. 3).

Remark 3.5. Note that the necessity of (3.13) follows from [10].
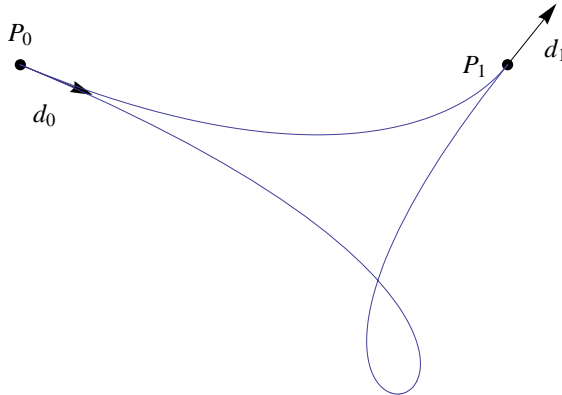
FIGURE 3. The data where two Hermite interpolating PH cubic curves exist.

By using the introduced notation it is easy to give an explicit form of the square root of the hodograph. Furthermore, a nice explicit formula for a reparameterization by a natural parameter can be obtained.

Theorem 3.6. *Suppose that the suppositions of Theorem 3.3 hold, and let the Hermite interpolating PH cubic curve $\boldsymbol{B}$ be determined by* (3.14). *The square root of its hodograph is*

$$(3.15) \qquad \sqrt{\boldsymbol{B}'(t)\cdot\boldsymbol{B}'(t)} = C_1 B_{2,0}(t) + C_2 B_{2,1}(t) + C_3 B_{2,2}(t),$$

where

$$C_1 := 3\lambda_0, \quad C_2 := \frac{3}{2}\left((\boldsymbol{d}_0 + \boldsymbol{d}_1)\cdot\Delta\boldsymbol{P}_0 - (\lambda_0 + \lambda_1)(1 + \boldsymbol{d}_0\cdot\boldsymbol{d}_1)\right), \quad C_3 := 3\lambda_1.$$

The arc-length reparameterization

$$\Phi := \Phi(\boldsymbol{d}_0, \Delta\boldsymbol{P}_0, \boldsymbol{d}_1) : [0, L] \to [0, 1],$$

where $L := 1/3\,(C_1 + C_2 + C_3)$ is the length of $\boldsymbol{B}$, is given by

$$(3.16) \qquad \Phi(s) = \frac{C_1 - C_2 + \sqrt[3]{\frac{2}{c_1(s)}}\left(C_1 C_3 - C_2^2\right) - \sqrt[3]{\frac{c_1(s)}{2}}}{C_1 - 2C_2 + C_3},$$

where

$$c_1(s) := c_2(s) + \sqrt{4\left(C_1 C_3 - C_2^2\right)^3 + c_2^2(s)},$$

$$c_2(s) := (C_1 - C_2)\left((C_1 - C_2)^2 + 3\left(C_1 C_3 - C_2^2\right)\right) - 3\left(C_1 - 2C_2 + C_3\right)^2 s.$$

Proof. With some algebraic computations and the use of (3.4), (3.5) and (3.6) one can verify that (3.15) holds. Then the arc-length s of the Bézier curve $\boldsymbol{B}$ is computed as

$$s = s(t) = \int_0^t \sqrt{\boldsymbol{B}'(u)\cdot\boldsymbol{B}'(u)}\, du, \quad t \in [0, 1].$$

Since by [3]

(3.17) $$\sqrt{\boldsymbol{B}'(t)\cdot\boldsymbol{B}'(t)} > 0,$$

s is a monotone function of t and thus invertible. The inverse $t = t(s) = \Phi(s)$, given by (3.16), is computed as a solution of a cubic equation

$$\frac{1}{3}(C_1 - 2C_2 + C_3)t^3 + (C_2 - C_1)t^2 + C_1 t = s.$$

Since there is only one real solution, we need to check that (3.16) is real. The inequality (3.17) and the fact, that a circle can not be parameterized by polynomials, imply $C_1 - 2C_2 + C_3 > 0$ and $C_1 C_3 - C_2^2 > 0$. Therefore it is clear that $c_1(s) > 0$ and the assertion follows. $\square$

4. INDUCTIVE STEP OF THE PROOF

In this section, an inductive proof of Theorem 2.1 will be given. The first step of the induction, the single segment case, has already been confirmed by Theorem 3.3. So, let us assume that there exist cubic PH G^2-continuous splines which interpolate the data

$$\boldsymbol{d}_0, \boldsymbol{P}_0, \boldsymbol{P}_1, \ldots, \boldsymbol{P}_\ell, \boldsymbol{d}_\ell,$$

and

$$\boldsymbol{d}_\ell, \boldsymbol{P}_\ell, \boldsymbol{P}_{\ell+1}, \ldots, \boldsymbol{P}_m, \boldsymbol{d}_m,$$

respectively, for any direction $\boldsymbol{d}_\ell$ in the cone, determined by $\Delta\boldsymbol{P}_{\ell-1}$ and $\Delta\boldsymbol{P}_\ell$. We have to show that there exists a unique direction $\boldsymbol{d}_\ell$ for which the splines have a G^2 joint. Consider the equation (2.7) at $\boldsymbol{P}_\ell$. Since a rotation preserves it, we may choose the coordinate system in such a way that
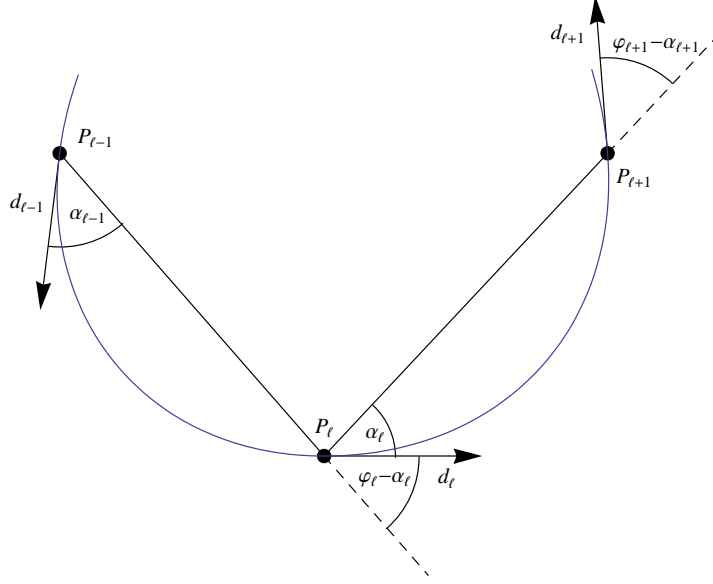
(4.1) $$\boldsymbol{d}_\ell = \begin{bmatrix} 1 \\ 0 \end{bmatrix}.$$

Further, as shown in Fig. 4,

$$\frac{1}{\|\Delta\boldsymbol{P}_{\ell-1}\|}\Delta\boldsymbol{P}_{\ell-1} = \begin{bmatrix} \cos(\varphi_\ell - \alpha_\ell) \\ -\sin(\varphi_\ell - \alpha_\ell) \end{bmatrix}, \quad \frac{1}{\|\Delta\boldsymbol{P}_\ell\|}\Delta\boldsymbol{P}_\ell = \begin{bmatrix} \cos\alpha_\ell \\ \sin\alpha_\ell \end{bmatrix},$$

and

$$\boldsymbol{d}_{\ell-1} = \begin{bmatrix} \cos(\varphi_\ell - \alpha_\ell + \alpha_{\ell-1}) \\ -\sin(\varphi_\ell - \alpha_\ell + \alpha_{\ell-1}) \end{bmatrix}, \quad \boldsymbol{d}_{\ell+1} = \begin{bmatrix} \cos(\alpha_\ell + \varphi_{\ell+1} - \alpha_{\ell+1}) \\ \sin(\alpha_\ell + \varphi_{\ell+1} - \alpha_{\ell+1}) \end{bmatrix}.$$

FIGURE 4. Joining two G^2-continuous cubic PH splines at $\boldsymbol{P}_\ell$.

The assumption (4.1) reduces the curvature condition (2.7) to the requirement that the last components of vectors

$$(4.2) \quad \frac{1}{\lambda_{2\ell}^2}\Delta\boldsymbol{P}_\ell - \frac{\lambda_{2\ell+1}}{\lambda_{2\ell}^2}\boldsymbol{d}_{\ell+1} = \frac{1}{\|\Delta\boldsymbol{P}_\ell\|}\left(\frac{\|\Delta\boldsymbol{P}_\ell\|}{\lambda_{2\ell}}\right)^2\left(\frac{\Delta\boldsymbol{P}_\ell}{\|\Delta\boldsymbol{P}_\ell\|} - \frac{\lambda_{2\ell+1}}{\|\Delta\boldsymbol{P}_\ell\|}\boldsymbol{d}_{\ell+1}\right),$$

and

$$(4.3) \quad -\frac{1}{\lambda_{2\ell-1}^2}\Delta\boldsymbol{P}_{\ell-1} + \frac{\lambda_{2\ell-2}}{\lambda_{2\ell-1}^2}\boldsymbol{d}_{\ell-1} =$$

$$= \frac{1}{\|\Delta\boldsymbol{P}_{\ell-1}\|}\left(\frac{\|\Delta\boldsymbol{P}_{\ell-1}\|}{\lambda_{2\ell-1}}\right)^2\left(-\frac{\Delta\boldsymbol{P}_{\ell-1}}{\|\Delta\boldsymbol{P}_{\ell-1}\|} + \frac{\lambda_{2\ell-2}}{\|\Delta\boldsymbol{P}_{\ell-1}\|}\boldsymbol{d}_{\ell-1}\right)$$

are equal. A straightforward algebraic simplification, with the help of (3.8) and the functions

$$\eta(\gamma,\delta) := \sqrt{1 + 6\frac{\sin\gamma\sin\delta}{1 - \cos(\gamma+\delta)}},$$

$$\chi(\gamma,\delta) := \frac{(\cos(\gamma-\delta)-1)\sin(\gamma+\delta) + (1-\cos(\gamma+\delta))(\sin\gamma+\sin\delta)\eta(\gamma,\delta)}{2(1-\cos(\gamma+\delta))(2(\cos\gamma+\cos\delta)+\eta(\gamma,\delta))},$$

$$\rho(\gamma,\delta) := \frac{3 - \cos\gamma\cos\delta - 2\cos(2\delta) + 3\sin\gamma\sin\delta + (\cos\gamma-\cos\delta)\eta(\gamma,\delta)}{2(1-\cos(\gamma+\delta))(2(\cos\gamma+\cos\delta)+\eta(\gamma,\delta))},$$

reveals the G^2-continuity condition expressed by (4.2) and (4.3) as

$$(4.4) \quad \frac{1}{\|\Delta\boldsymbol{P}_\ell\|}\frac{\chi(\alpha_\ell, \varphi_{\ell+1}-\alpha_{\ell+1})}{\rho^2(\alpha_\ell, \varphi_{\ell+1}-\alpha_{\ell+1})} = \frac{1}{\|\Delta\boldsymbol{P}_{\ell-1}\|}\frac{\chi(\varphi_\ell-\alpha_\ell, \alpha_{\ell-1})}{\rho^2(\varphi_\ell-\alpha_\ell, \alpha_{\ell-1})}.$$

Note that $\rho(\alpha_\ell, \varphi_{\ell+1} - \alpha_{\ell+1}) = \Lambda_0^+ \left(\boldsymbol{d}_\ell, \Delta \boldsymbol{P}_\ell, \boldsymbol{d}_{\ell+1} \right) / \|\Delta \boldsymbol{P}_\ell\|$, and $\chi(\alpha_\ell, \varphi_{\ell+1} - \alpha_{\ell+1})$ corresponds to the last component of

$$\frac{\Delta \boldsymbol{P}_\ell}{\|\Delta \boldsymbol{P}_\ell\|} - \frac{\Lambda_1^+ \left(\boldsymbol{d}_\ell, \Delta \boldsymbol{P}_\ell, \boldsymbol{d}_{\ell+1} \right)}{\|\Delta \boldsymbol{P}_\ell\|} \boldsymbol{d}_{\ell+1},$$

and similarly for the right hand side of (4.4). Let

$$\omega(\alpha, \beta, \gamma, \delta) := \frac{\chi(\alpha, \gamma)}{\rho^2(\alpha, \gamma)} \frac{\rho^2(\beta, \delta)}{\chi(\beta, \delta)}.$$

We are looking for $\alpha_\ell \in (0, \varphi_\ell)$ that satisfies

$$(4.5) \qquad \omega(\alpha_\ell) := \omega(\alpha_\ell, \varphi_\ell - \alpha_\ell, \varphi_{\ell+1} - \alpha_{\ell+1}, \alpha_{\ell-1}) = \frac{\|\Delta \boldsymbol{P}_\ell\|}{\|\Delta \boldsymbol{P}_{\ell-1}\|},$$

with the following requirements met by the data and the neighbouring tangent directions

$$0 < \varphi_{\ell-1} < \pi, \quad 0 < \varphi_\ell < \pi, \quad 0 < \varphi_{\ell+1} < \pi,$$

$$(4.6) \qquad \varphi_{\ell-1} + \varphi_\ell < \frac{4}{3}\pi, \quad \varphi_\ell + \varphi_{\ell+1} < \frac{4}{3}\pi,$$

$$0 < \alpha_{\ell-1} < \varphi_{\ell-1}, \quad 0 < \alpha_{\ell+1} < \varphi_{\ell+1}.$$

By Theorem 3.3, the conditions (4.6) imply

$$\rho(\alpha_\ell, \varphi_{\ell+1} - \alpha_{\ell+1}) > 0, \quad \rho(\varphi_\ell - \alpha_\ell, \alpha_{\ell-1}) > 0, \quad 0 < \alpha_\ell < \varphi_\ell,$$

and

$$\chi(\alpha_\ell, \varphi_{\ell+1} - \alpha_{\ell+1}) > 0, \quad 0 < \alpha_\ell < \varphi_\ell, \quad \chi(\varphi_\ell - \alpha_\ell, \alpha_{\ell-1}) > 0, \quad 0 < \alpha_\ell < \varphi_\ell.$$

So, ω is a continuous, even smooth function in (4.6). Further, from the expansions

$$\omega(\alpha_\ell) = \alpha_\ell \frac{\rho^2(\varphi_\ell, \alpha_{\ell-1})}{\chi(\varphi_\ell, \alpha_{\ell-1})} + \mathcal{O}\left(\alpha_\ell^2\right),$$

$$\omega(\alpha_\ell) = \frac{1}{\varphi_\ell - \alpha_\ell} \frac{\chi(\varphi_\ell, \varphi_{\ell+1} - \alpha_{\ell+1})}{\rho^2(\varphi_\ell, \varphi_{\ell+1} - \alpha_{\ell+1})} + \mathcal{O}\left((\varphi_\ell - \alpha_\ell)^0\right),$$

we conclude that the equation (4.5) has a solution $\alpha_\ell \in (0, \varphi_\ell)$. In order to show that this solution is unique, it is enough to prove monotonicity too. In general,
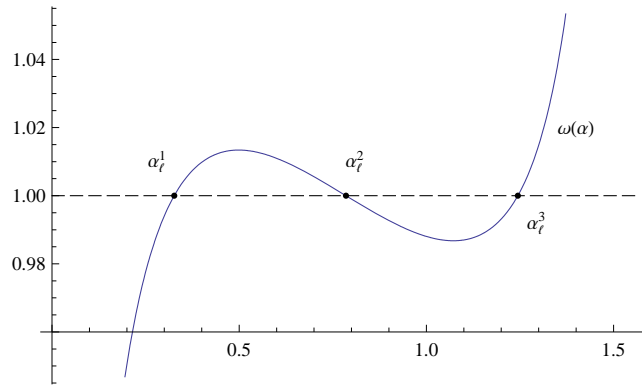

FIGURE 5. An example of $\omega = \omega(\alpha_\ell)$ that admits three solutions.

there may be multiple solutions. For example, data

$$\varphi_\ell = \frac{\pi}{2}, \ \varphi_{\ell+1} - \alpha_{\ell+1} = \alpha_{\ell-1} = \frac{41}{50}\pi$$

clearly give three solutions if $\|\Delta \boldsymbol{P}_\ell\| = \|\Delta \boldsymbol{P}_{\ell-1}\| = 1$ (Fig. 5, and Fig. 6),

$$\alpha_\ell^1 = 0.326428, \quad \alpha_\ell^2 = 0.785398, \quad \alpha_\ell^3 = 1.24437.$$

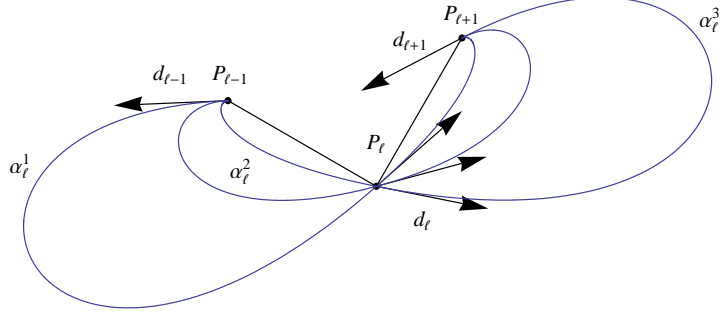Thus an additional restriction as assumed in Theorem 2.1 is necessary, which

FIGURE 6. Three admissible solutions ($\alpha_\ell = 0.326428, 0.785398, 1.24437$).

strengthens the bounds (4.6) imposed on the data by

(4.7) $$0 < \varphi_{\ell-1} + \varphi_\ell < K\pi, \quad 0 < \varphi_\ell + \varphi_{\ell+1} < K\pi.$$

It is enough to consider the monotonicity of $\ln\omega$ only. Its derivative is given as

$$\frac{d}{d\alpha_\ell} \ln\omega(\alpha_\ell) = \tau(\alpha_\ell, \varphi_{\ell+1} - \alpha_{\ell+1}) + \tau(\varphi_\ell - \alpha_\ell, \alpha_{\ell-1}),$$

where

$$\tau(\gamma, \delta) := \frac{\frac{\partial}{\partial\gamma}\chi(\gamma,\delta)}{\chi(\gamma,\delta)} - 2\frac{\frac{\partial}{\partial\gamma}\rho(\gamma,\delta)}{\rho(\gamma,\delta)}.$$

The complete expression τ is rather long,

$$\tau(\gamma,\delta) = \cot\frac{\gamma+\delta}{2} +$$

$$+ \frac{3\sin(\gamma-\delta)\sin\delta +}{\eta(\gamma,\delta)((1-\cos(\gamma-\delta))\sin(\gamma+\delta) + (\cos(\gamma+\delta)-1)(\sin\gamma+\sin\delta)\eta(\gamma,\delta))}$$

$$\frac{+\eta(\gamma,\delta)\left(-2(2\cos\gamma+\cos\delta)\eta(\gamma,\delta)\sin^2\frac{\gamma+\delta}{2} - \cos 2\gamma + \cos(\gamma+\delta)\right)}{.} +$$

$$+ \frac{3\dfrac{(\cos\gamma-\cos\delta)\sin\delta}{(\cos(\gamma+\delta)-1)^2\eta(\gamma,\delta)} - 2\sin(\gamma)}{2(\cos\gamma+\cos\delta)+\eta(\gamma,\delta)} +$$

$$+ 2\frac{3\dfrac{\sin\delta(\cos\gamma-\cos\delta)^2}{(\cos(\gamma+\delta)-1)^2\eta(\gamma,\delta)} + \cos\delta\sin\gamma + 3\cos\gamma\sin\delta - \sin\gamma\,\eta(\gamma,\delta)}{2\cos 2\delta - 3\sin\gamma\sin\delta - \cos\gamma\,\eta(\gamma,\delta) + \cos\delta\,(\cos\gamma + \eta(\gamma,\delta)) - 3},$$

but one can establish that it is decreasing in the variable δ if both parameters belong to the domain

$$D_\tau = \left\{ (\gamma, \delta) : 0 < \gamma \leq \frac{\pi}{3}, \ 0 < \delta < \pi \right\} \cup \left\{ (\gamma, \delta) : \frac{\pi}{3} < \gamma < \pi, \ 0 < \delta < \frac{4\pi}{3} - \gamma \right\}.$$

Let us prove that $\tau_\delta := \dfrac{\partial \tau}{\partial \delta}$ is negative on D_τ. At the boundary of D_τ the following
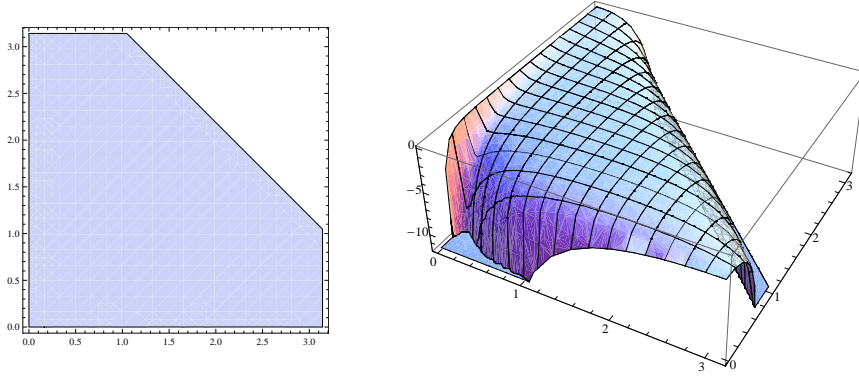

FIGURE 7. The domain D_τ and the behaviour of the function $\tau_\delta(\gamma, \delta)$ on D_τ.

hold true,

$$\tau_\delta(\gamma, \delta) = -6\,\gamma\,\frac{\cos\frac{\delta}{2}}{\sin^3\frac{\delta}{2}} + \mathcal{O}\left(\gamma\right) < 0, \qquad\qquad\qquad 0 < \delta < \pi,$$

$$\tau_\delta(\gamma, \delta) = -\frac{3}{\sin^2\frac{\gamma}{2}} + \mathcal{O}\left(\delta\right) < 0, \qquad\qquad\qquad 0 < \gamma < \pi,$$

$$\tau_\delta(\gamma, \delta) = -18\,\frac{\cos\gamma\,\sin^2\frac{\gamma}{2}}{\cos^2\frac{3\gamma}{2}} + \mathcal{O}\left(\pi - \delta\right) < 0, \qquad\qquad 0 < \gamma \leq \frac{\pi}{3},$$

$$\tau_\delta(\gamma, \delta) = -\frac{3}{2}\,\frac{\left((\cos\delta - 1)^2 + \cos^2\delta + 1\right)}{\cos^2\frac{3\delta}{2}} + \mathcal{O}\left(\pi - \gamma\right) < 0, \qquad 0 < \delta < \frac{\pi}{3}.$$

Further, if $\delta \to \frac{4\pi}{3} - \gamma$ and $\frac{\pi}{3} < \gamma < \pi$, then $\tau_\delta(\gamma, \delta) \to -\infty$. This shows that τ_δ is negative near the boundary. A direct numerical evaluation confirms this fact for all $(\gamma, \delta) \in D_\tau$. More precisely, the maximum of τ_δ on D_τ is zero, and it is attained at the boundary $\gamma = 0$ (see Fig. 7). Therefrom for data satisfying (4.7) we obtain the following estimations. If $0 < \varphi_\ell \leq \frac{\pi}{3}$, then

$$\tau(\alpha_\ell, \varphi_{\ell+1} - \alpha_{\ell+1}) + \tau(\varphi_\ell - \alpha_\ell, \alpha_{\ell-1}) \geq \tau(\alpha_\ell, \pi) + \tau(\varphi_\ell - \alpha_\ell, \pi) =: \Psi_1(\alpha_\ell, \varphi_\ell),$$

and if $\frac{\pi}{3} < \varphi_\ell < \pi$, then

$$\tau(\alpha_\ell, \varphi_{\ell+1} - \alpha_{\ell+1}) + \tau(\varphi_\ell - \alpha_\ell, \alpha_{\ell-1}) \geq \tau(\alpha_\ell, K\pi - \varphi_\ell) + \tau(\varphi_\ell - \alpha_\ell, K\pi - \varphi_\ell)$$
$$=: \Psi_K(\alpha_\ell, \varphi_\ell).$$

We need to show that Ψ_1 and Ψ_K are nonnegative on D_1 and D_2 respectively, where

$$D_1 = \left\{ (\alpha_\ell, \varphi_\ell) : \ 0 < \alpha_\ell < \varphi_\ell, \ 0 < \varphi_\ell \leq \frac{\pi}{3} \right\},$$

$$D_2 = \left\{ (\alpha_\ell, \varphi_\ell) : \ 0 < \alpha_\ell < \varphi_\ell, \ \frac{\pi}{3} < \varphi_\ell < \pi \right\}.$$

One can verify that the global minimum of Ψ_1 is $\sqrt{3} - 1$ and it is reached on the boundary in the point $(\alpha_\ell, \varphi_\ell) = \left(\frac{\pi}{6}, \frac{\pi}{3} \right)$. The global minimum of Ψ_K is zero, reached in the interior stationary point $(\alpha_\ell, \varphi_\ell) = ((K-1)\pi, 2(K-1)\pi)$ (see Fig. 8). It is easy to check that for any $\tilde{K}$, $K < \tilde{K} < \frac{4}{3}$, $\Psi_{\tilde{K}}$ attains negative
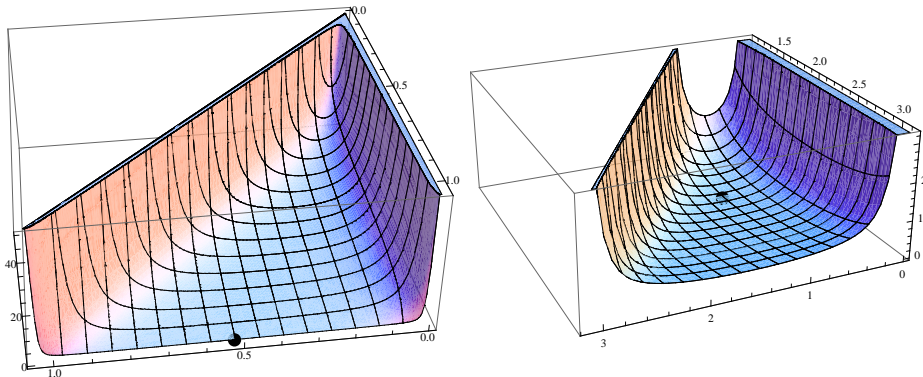

FIGURE 8. Plots of Ψ_1 and Ψ_K on D_1 and D_2, respectively, with a marked global minimum.

values in D_2. So K is the best constant bound we can get. From the other point of view, the meaning of K is the following. For $\varphi_\ell = 2(K-1)\pi$, the derivative of $\omega(\alpha_\ell, \varphi_\ell - \alpha_\ell, K\pi - \varphi_\ell, K\pi - \varphi_\ell)$ has a double zero in $\alpha_\ell = \frac{\varphi_\ell}{2}$, and further, $\omega(\alpha_\ell, \varphi_\ell - \alpha_\ell, (K + \epsilon_1)\pi - \varphi_\ell, (K + \epsilon_2)\pi - \varphi_\ell)$ is not a monotone function for any $\epsilon_1, \epsilon_2 \in \left(0, \frac{4}{3} - K \right)$.

5. APPROXIMATION ORDER

Let us now consider the asymptotic behaviour of the system (2.7). For this purpose, we assume that data are sampled from a smooth convex curve $\boldsymbol{f} : [0, h] \to \mathbb{R}^2$, parameterised by the arclength. Further, let the data points be determined by the partition

$$0 = \mu_0 < \mu_1 < \cdots < \mu_m = h,$$

with a bounded global mesh ratio. Namely,

$$\boldsymbol{P}_\ell = \boldsymbol{f}(\mu_\ell), \quad \ell = 0, 1, \ldots, m,$$

and similarly for the derivatives at the boundary. So, with

(5.1) $$\Delta \mu_\ell =: \nu_\ell \, h,$$

for some constant const > 0,

(5.2) $$\sup_{i,j} \frac{\nu_i}{\nu_j} \leq \text{const} < \infty.$$

Let us now show that the unknown directions $\boldsymbol{d}_\ell$ that satisfy the system (2.7) can be looked for as

(5.3) $$\boldsymbol{d}_\ell = Q(-h^3\, u_\ell)\boldsymbol{f}'\,(\mu_\ell)\,, \quad \ell = 1, 2, \ldots, m-1,$$

for all h small enough. Here, Q denotes the rotation matrix

$$Q(\varphi) = \begin{bmatrix} \cos\varphi & -\sin\varphi \\ \sin\varphi & \cos\varphi \end{bmatrix},$$

and u_ℓ are unknowns to be determined by the system (2.7). Let us expand the equation of this system at a particular index ℓ. Some simplifications can be done in advance. The equation concerned is obviously independent of a translation of the coordinate system. Also, in view of Section 3, a rotation does not change the values of λ_j. Let Q_ℓ denote the rotation matrix that brings $\boldsymbol{d}_\ell$ to $\boldsymbol{e}_1 := [1, 0]^T$. The equation $\boldsymbol{e}_1 \times \boldsymbol{q}_\ell = 0$, where

(5.4) $$\boldsymbol{q}_\ell := \left(\frac{1}{\lambda_{2\ell}^2} Q_\ell \Delta \boldsymbol{P}_\ell + \frac{1}{\lambda_{2\ell-1}^2} Q_\ell \Delta \boldsymbol{P}_{\ell-1} \right) - \frac{\lambda_{2\ell-2}}{\lambda_{2\ell-1}^2} Q_\ell \boldsymbol{d}_{\ell-1} - \frac{\lambda_{2\ell+1}}{\lambda_{2\ell}^2} Q_\ell \boldsymbol{d}_{\ell+1},$$

is equivalent to the original one. But this is the same as to require that the second component of the vector $\boldsymbol{q}_\ell$ vanishes, i.e.,

(5.5) $$\left(\frac{1}{\|\boldsymbol{q}_\ell\|} \boldsymbol{q}_\ell \right)_2 = 0.$$

The assumption (5.3) implies that Q_ℓ can be written as a product of rotations

$$Q_\ell = \tilde{Q}_\ell Q^T(-h^3\, u_\ell) = \tilde{Q}_\ell Q(h^3\, u_\ell), \quad \text{with} \quad \tilde{Q}_\ell \boldsymbol{f}'\,(\mu_\ell) = \boldsymbol{e}_1.$$

Since rotations in $\mathbb{R}^2$ commute, the vectors in (5.4) can be simplified to

(5.6) $$Q_\ell \Delta \boldsymbol{P}_\ell = Q(h^3\, u_\ell) \left(\tilde{Q}_\ell \Delta \boldsymbol{P}_\ell \right), \quad Q_\ell \Delta \boldsymbol{P}_{\ell-1} = Q(h^3\, u_\ell) \left(\tilde{Q}_\ell \Delta \boldsymbol{P}_{\ell-1} \right),$$

and

(5.7) $$Q_\ell \boldsymbol{d}_{\ell\pm1} = Q(h^3\, (u_\ell - u_{\ell\pm1})) \left(\tilde{Q}_\ell \boldsymbol{f}'(\mu_{\ell\pm1}) \right).$$

This shows that the asymptotic behaviour of the equation (5.5) can be studied with $\boldsymbol{f}$ expanded locally as $\boldsymbol{g}_\ell$,

$$\boldsymbol{g}_\ell(s) := \tilde{Q}_\ell \left(\boldsymbol{f}(\mu_\ell + s) - \boldsymbol{P}_\ell \right), \quad s \in [-\nu_{\ell-1}h, \nu_\ell h],$$

at each ℓ separately. Since the parameter s is the arclength, we may assume that the tangent direction is given as

$$\boldsymbol{g}'_\ell(s) = \begin{bmatrix} \cos\theta_\ell(s) \\ \sin\theta_\ell(s) \end{bmatrix},$$

where $\theta'_\ell(s) > 0$ is the curvature of $\boldsymbol{f}$. An expansion

$$\theta_\ell(s) = \theta_{\ell,1}s + \theta_{\ell,2}s^2 + \theta_{\ell,3}s^3 + \theta_{\ell,4}s^4 + \mathcal{O}\left(s^5\right)$$

yields

$$\boldsymbol{g}_\ell(s) = \begin{bmatrix} s - \frac{1}{6}\theta_{\ell,1}^2 s^3 - \frac{1}{4}\theta_{\ell,1}\theta_{\ell,2}s^4 + \frac{1}{120}\left(\theta_{\ell,1}^4 - 24\theta_{\ell,3}\theta_{\ell,1} - 12\theta_{\ell,2}^2\right)s^5 \\ \frac{\theta_{\ell,1}}{2}s^2 + \frac{\theta_{\ell,2}}{3}s^3 + \frac{1}{24}\left(6\theta_{\ell,3} - \theta_{\ell,1}^3\right)s^4 + \frac{1}{10}\left(2\theta_{\ell,4} - \theta_{\ell,1}^2\theta_{\ell,2}\right)s^5 \end{bmatrix} + \mathcal{O}\left(s^6\right).$$

Note that $\theta_{\ell,1} > 0$ by the assumption. Since the rotation matrices needed expand as

$$Q\left(u\,s^3\right) = \begin{bmatrix} 1 - \frac{1}{2}u^2\,s^6 & -u\,s^3 \\ u\,s^3 & 1 - \frac{1}{2}u^2\,s^6 \end{bmatrix} + \mathcal{O}\left(s^8\right),$$

it is straightforward to compute the expansions (5.6) and (5.7). Further, by inserting these expansions in λ_i, one obtains

(5.8) $\lambda_{2\ell-2} = \dfrac{\nu_{\ell-1}}{3}h + \dfrac{\nu_{\ell-1}^2\theta_{\ell,2}}{6\theta_{\ell,1}}h^2 +$

$$+ \frac{\left(\theta_{\ell,1}^4 - 18\theta_{\ell,3}\theta_{\ell,1} + 13\theta_{\ell,2}^2\right)\nu_{\ell-1}^3 - 36\theta_{\ell,1}(u_{\ell-1} + u_\ell)}{72\theta_{\ell,1}^2}h^3 + \mathcal{O}\left(h^4\right),$$

(5.9) $\lambda_{2\ell-1} = \dfrac{\nu_{\ell-1}}{3}h - \dfrac{\nu_{\ell-1}^2\theta_{\ell,2}}{6\theta_{\ell,1}}h^2 +$

$$+ \frac{\left(\theta_{\ell,1}^4 + 18\theta_{\ell,3}\theta_{\ell,1} - 11\theta_{\ell,2}^2\right)\nu_{\ell-1}^3 + 36\theta_{\ell,1}(u_{\ell-1} + u_\ell)}{72\theta_{\ell,1}^2}h^3 + \mathcal{O}\left(h^4\right),$$

$\lambda_{2\ell} = \dfrac{\nu_\ell}{3}h + \dfrac{\nu_\ell^2\theta_{\ell,2}}{6\theta_{\ell,1}}h^2 +$

$$+ \frac{\left(\theta_{\ell,1}^4 + 18\theta_{\ell,3}\theta_{\ell,1} - 11\theta_{\ell,2}^2\right)\nu_\ell^3 - 36\theta_{\ell,1}(u_\ell + u_{\ell+1})}{72\theta_{\ell,1}^2}h^3 + \mathcal{O}\left(h^4\right),$$

$\lambda_{2\ell+1} = \dfrac{\nu_\ell}{3}h - \dfrac{\nu_\ell^2\theta_{\ell,2}}{6\theta_{\ell,1}}h^2 +$

$$+ \frac{\left(\theta_{\ell,1}^4 - 18\theta_{\ell,3}\theta_{\ell,1} + 13\theta_{\ell,2}^2\right)\nu_\ell^3 + 36\theta_{\ell,1}(u_\ell + u_{\ell+1})}{72\theta_{\ell,1}^2}h^3 + \mathcal{O}\left(h^4\right).$$

Let us apply the obtained expansions in (5.5). The system of equations for h small enough reads

$$\frac{\nu_\ell}{2\left(\nu_{\ell-1} + \nu_\ell\right)}u_{\ell-1} + u_\ell + \frac{\nu_{\ell-1}}{2\left(\nu_{\ell-1} + \nu_\ell\right)}u_{\ell+1} =$$

$$= \frac{\nu_{\ell-1}\left(\nu_{\ell-1} - \nu_\ell\right)\nu_\ell\left(\theta_{\ell,1}^4 + 6\theta_{\ell,3}\theta_{\ell,1} - 7\theta_{\ell,2}^2\right)}{48\theta_{\ell,1}} + \mathcal{O}\left(h\right),$$

(5.10) $\qquad\qquad\qquad\qquad\qquad \ell = 1, 2, \ldots, m-1.$

The matrix involved in the system (5.10) has been around for quite a while, and appears in the cubic spline interpolation (see for example [2] and the references therein). It is strictly diagonally dominant, totally positive, etc. As a consequence, a unique (and by (5.2) bounded) solution of the system (5.10) exists for all h small enough. The unknowns that satisfy the system are of the form

$$u_\ell = \text{const}_\ell + \mathcal{O}\left(h\right), \quad \ell = 1, 2, \ldots, m-1.$$

We are now ready to prove that the asymptotic approximation order is 4. It is enough to show that this is true for any segment $\boldsymbol{B}^\ell$ of the spline curve. Thus let $\boldsymbol{B}^\ell$ be an ℓ-th segment of the interpolating G^2 cubic PH spline defined by (2.3),

and let $\boldsymbol{H}^\ell$ be the standard cubic C^1 Hermite interpolant of $\boldsymbol{f}|_{[\mu_{\ell-1},\mu_\ell]}$, i.e.,

$$\boldsymbol{H}^\ell(\mu_i) = \boldsymbol{f}(\mu_i), \quad i = \ell - 1, \ell,$$

$$\frac{d}{ds}\boldsymbol{H}^\ell(\mu_i) = \frac{d}{ds}\boldsymbol{f}(\mu_i) =: \boldsymbol{f}'(\mu_i), \quad i = \ell - 1, \ell.$$

The distance $\mathrm{dist}\left(\boldsymbol{f}|_{[\mu_{\ell-1},\mu_\ell]}, \boldsymbol{B}^\ell\right)$ is clearly bounded as

$$\mathrm{dist}\left(\boldsymbol{f}|_{[\mu_{\ell-1},\mu_\ell]}, \boldsymbol{B}^\ell\right) \le \mathrm{dist}\left(\boldsymbol{f}|_{[\mu_{\ell-1},\mu_\ell]}, \boldsymbol{H}^\ell\right) + \mathrm{dist}\left(\boldsymbol{H}^\ell, \boldsymbol{B}^\ell\right)$$

$$\le \max_{s\in[\mu_{\ell-1},\mu_\ell]}\left\|\boldsymbol{f}(s) - \boldsymbol{H}^\ell(s)\right\| + \max_{s\in[\mu_{\ell-1},\mu_\ell]}\left\|\boldsymbol{H}^\ell(s) - \boldsymbol{B}^\ell(\phi_\ell(s))\right\|,$$

where, without loosing generality, ϕ_ℓ might be chosen as

$$\phi_\ell(s) := \frac{1}{\Delta\mu_{\ell-1}}(s - \mu_{\ell-1}).$$

A very well known result on Hermite interpolation and (5.1) lead to

$$\max_{s\in[\mu_{\ell-1},\mu_\ell]}\left\|\boldsymbol{f}(s) - \boldsymbol{H}^\ell(s)\right\| = \mathcal{O}\left((\Delta\mu_{\ell-1})^4\right) = \mathcal{O}\left((\nu_{\ell-1}\,h)^4\right) = \mathcal{O}\left(h^4\right).$$

Thus it remains to prove that $\max_{s\in[\mu_{\ell-1},\mu_\ell]}\left\|\boldsymbol{H}^\ell(s) - \boldsymbol{B}^\ell(\phi_\ell(s))\right\| = \mathcal{O}\left(h^4\right)$. It is well known that $\boldsymbol{H}^\ell$ can be written in the Bézier form as

$$\boldsymbol{H}^\ell(s) = \boldsymbol{f}(\mu_{\ell-1})\,B_{3,0}(\tau) + \left(\boldsymbol{f}(\mu_{\ell-1}) + \frac{\Delta\mu_{\ell-1}}{3}\boldsymbol{f}'(\mu_{\ell-1})\right)B_{3,1}(\tau) +$$

$$+ \left(\boldsymbol{f}(\mu_\ell) - \frac{\Delta\mu_{\ell-1}}{3}\boldsymbol{f}'(\mu_\ell)\right)B_{3,2}(\tau) + \boldsymbol{f}(\mu_\ell)\,B_{3,3}(\tau),\ \tau = \frac{s - \mu_{\ell-1}}{\Delta\mu_{\ell-1}},\ s\in[\mu_{\ell-1},\mu_\ell].$$

On the other hand, (2.6) implies

$$\boldsymbol{B}^\ell(\phi_\ell(s)) = \boldsymbol{f}(\mu_{\ell-1})\,B_{3,0}(\tau) + (\boldsymbol{f}(\mu_{\ell-1}) + \lambda_{2\,\ell-2}\boldsymbol{d}_{\ell-1})\,B_{3,1}(\tau) +$$

$$+ (\boldsymbol{f}(\mu_\ell) - \lambda_{2\,\ell-1}\boldsymbol{d}_\ell)\,B_{3,2}(\tau) + \boldsymbol{f}(\mu_\ell)\,B_{3,3}(\tau), \quad \tau = \frac{s - \mu_{\ell-1}}{\Delta\mu_{\ell-1}}, \quad s\in[\mu_{\ell-1},\mu_\ell].$$

Consequently,

$$\boldsymbol{H}^\ell(s) - \boldsymbol{B}^\ell(\phi_\ell(s)) =$$

$$= \left(\frac{\Delta\mu_{\ell-1}}{3}\boldsymbol{f}'(\mu_{\ell-1}) - \lambda_{2\,\ell-2}\boldsymbol{d}_{\ell-1}\right)B_{3,1}(\tau) + \left(\lambda_{2\,\ell-1}\boldsymbol{d}_\ell - \frac{\Delta\mu_{\ell-1}}{3}\boldsymbol{f}'(\mu_\ell)\right)B_{3,2}(\tau).$$

But by (5.3), $\boldsymbol{d}_i = \boldsymbol{f}'(\mu_i) + \mathcal{O}\left(h^3\right)$, $i = \ell - 1, \ell$. Using this together with (5.1), (5.8), (5.9) and the fact that u_i is bounded by a constant, leads to

$$\max_{s\in[\mu_{\ell-1},\mu_\ell]}\left\|\boldsymbol{H}^\ell(s) - \boldsymbol{B}^\ell(\phi_\ell(s))\right\| = \mathcal{O}\left(h^4\right).$$

Note that the first and the last segment should be analysed slightly differently, since tangent directions are prescribed there. But it is easy to see that the same results hold and we shall skip the details. This completes the proof.

6. NUMERICAL EXAMPLES AND PREPROCESSING ALGORITHM

An efficient and reliable numerical algorithm for convex data, satisfying the assumptions of Theorem 2.1 with the bound on the angles decreased to $K\pi$, can be obtained by using the continuation method. Note that the problem involves solving a tridiagonal system of nonlinear equations. Although all the examples were computed using this method, we suggest an alternative, computationally simpler approach. The algorithm iteratively computes the unknown tangent directions $\boldsymbol{d}_\ell$, $\ell = 1, 2, \ldots, m-1$, with

$$\boldsymbol{d}_\ell^{[0]} = \frac{\boldsymbol{P}_{\ell+1} - \boldsymbol{P}_{\ell-1}}{\|\boldsymbol{P}_{\ell+1} - \boldsymbol{P}_{\ell-1}\|}, \quad \ell = 1, 2, \ldots, m-1,$$

as the starting values. In the $(r+1)$-th iteration we first compute

$$\lambda_{2\ell} := \Lambda_0^+ \left(\boldsymbol{d}_\ell^{[r]}, \Delta\boldsymbol{P}_\ell, \boldsymbol{d}_{\ell+1}^{[r]}\right), \ \lambda_{2\ell+1} := \Lambda_1^+ \left(\boldsymbol{d}_\ell^{[r]}, \Delta\boldsymbol{P}_\ell, \boldsymbol{d}_{\ell+1}^{[r]}\right), \quad \ell = 0, 1, \ldots, m-1,$$

and then for $\ell = 1, 2, \ldots, m-1$,

$$\boldsymbol{d}_\ell^{[r+1]} = \left(\frac{1}{\lambda_{2\ell}^2}\left(\Delta\boldsymbol{P}_\ell - \lambda_{2\ell+1}\,\boldsymbol{d}_{\ell+1}^{[r]}\right) + \frac{1}{\lambda_{2\ell-1}^2}\left(\Delta\boldsymbol{P}_{\ell-1} - \lambda_{2\ell-2}\,\boldsymbol{d}_{\ell-1}^{[r]}\right)\right).$$

Here $\boldsymbol{d}_0^{[r]} = \boldsymbol{d}_0$ and $\boldsymbol{d}_m^{[r]} = \boldsymbol{d}_m$ for each r. Numerical evidence suggests that the procedure is reliable and convergent, but it seems hard to prove the convergence in general.

When closed splines are under consideration all tangent directions are unknown and the algorithm needs only slight modifications. An example of such an interpolant together with its curvature plot is shown in Fig. 9.
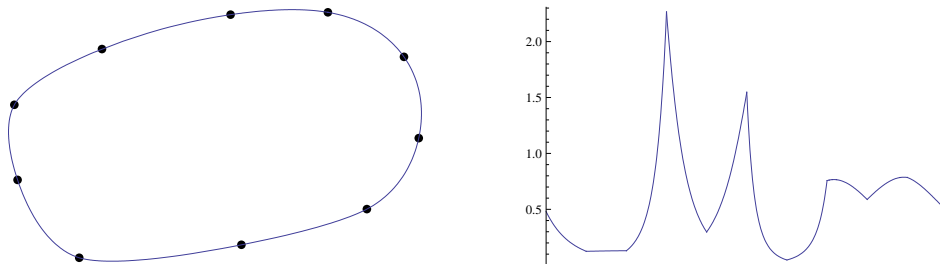

FIGURE 9. A closed cubic PH spline interpolant and its curvature.

But since for general data an interpolating cubic PH G^2 spline might not exist, a preprocessing algorithm must be considered first. Since convexity of the data is necessary for such a spline, an efficient split of the data into convex segments is needed. Thus an additional point has to be inserted, whenever an inflection point in the data polygon occurs (Fig. 10). Let $\boldsymbol{P}_{\ell-2}, \boldsymbol{P}_{\ell-1}, \boldsymbol{P}_\ell, \boldsymbol{P}_{\ell+1}$ be a nonconvex segment of data points. Then one possibility how to determine a new point $\boldsymbol{P}'$ and a new direction $\boldsymbol{d}'$ is to use the cubic polynomial curve which interpolates the given four data. The point $\boldsymbol{P}'$ can then be chosen as an intersection of the polynomial and the line segment $\boldsymbol{P}_{\ell-1}\boldsymbol{P}_\ell$, while an appropriate choice for the direction $\boldsymbol{d}'$ is to take a normalized tangent vector of the polynomial at $\boldsymbol{P}'$. If the intersection is empty, take $\boldsymbol{P}' = (\boldsymbol{P}_{\ell-1} + \boldsymbol{P}_\ell)/2$ and choose $\boldsymbol{d}'$ appropriately. Recall that we

have to restrict our requirements to G^1 continuity at the newly added points. The
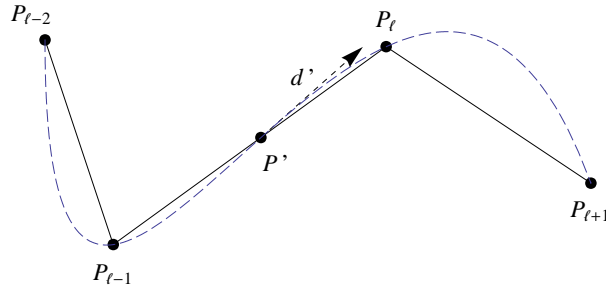

FIGURE 10. An insertion of an additional point in a locally non-convex segment.

data are now split into convex segments. But if for some convex segment any of the angles in Theorem 2.1 is greater than $K\pi$, the solution may not be unique or may not even exist on this segment. Thus an insertion of an additional point is necessary (Fig. 11). The following lemma, that needs no additional proving (see Fig. 11), and Remark 6.2 show that it suffices to add one additional point on each such segment, and suggest a way to do it.
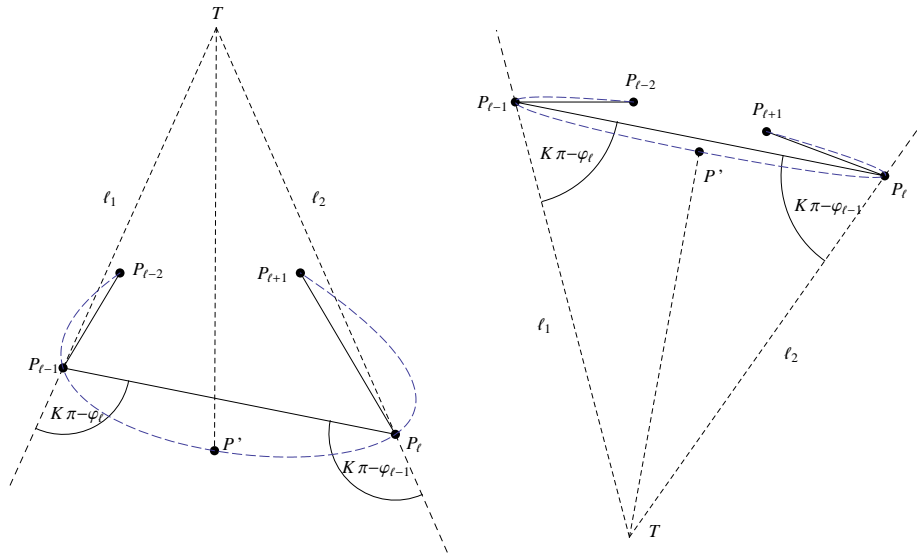

FIGURE 11. Two examples of the insertion of an additional point $\boldsymbol{P}'$ in a locally convex segment.

Lemma 6.1. *Let* $\boldsymbol{P}_{\ell-2}, \boldsymbol{P}_{\ell-1}, \boldsymbol{P}_\ell, \boldsymbol{P}_{\ell+1}$ *be convex data with*

$$\varphi_{\ell-1} + \varphi_\ell > K\pi,$$

and let $\boldsymbol{P}'$ *be any point inside the open domain* Ω, *bounded by the lines*

$$\ell_1(t) := \boldsymbol{P}_{\ell-1} + t\,Q(\varphi_\ell - (K-1)\pi)\Delta\boldsymbol{P}_{\ell-1}, \ \ell_2(t) := \boldsymbol{P}_\ell + t\,Q(K\pi - \varphi_{\ell-1})\Delta\boldsymbol{P}_{\ell-1},$$

and the half-plane determined by the line $\ell(t) := \boldsymbol{P}_{\ell-1} + t\Delta\boldsymbol{P}_{\ell-1}$ *not containing* $\boldsymbol{P}_{\ell-2}$ *and* $\boldsymbol{P}_{\ell+1}$. *Then*

$$\angle\left(\Delta\boldsymbol{P}_{\ell-2}, \boldsymbol{P}' - \boldsymbol{P}_{\ell-1}\right) + \angle\left(\boldsymbol{P}' - \boldsymbol{P}_{\ell-1}, \boldsymbol{P}_\ell - \boldsymbol{P}'\right) < K\pi,$$

and

$$\angle\left(\boldsymbol{P}' - \boldsymbol{P}_{\ell-1}, \boldsymbol{P}_\ell - \boldsymbol{P}'\right) + \angle\left(\boldsymbol{P}_\ell - \boldsymbol{P}', \Delta\boldsymbol{P}_\ell\right) < K\pi.$$

Remark 6.2. By the Bézout's theorem, the cubic polynomial curve which interpolates the data given in Lemma 6.1 does not form a loop and has no inflection points. Since usually the cubic interpolating polynomial intersects the domain Ω, an additional point $\boldsymbol{P}'$ can in this case be chosen as the intersection of the polynomial and the angle bisector at the point $\boldsymbol{T} := \ell_1 \cap \ell_2$ (see Fig. 11).

In Fig. 12, two examples, obtained by the presented preprocessing algorithm, are shown. Note that in the first example, there are only two additional points added by the preprocessing algorithm.

Finally, a comparison between a cubic G^2 PH spline and a classical cubic C^2 spline is shown in Fig. 13. Both splines have the same end-point tangent vectors.
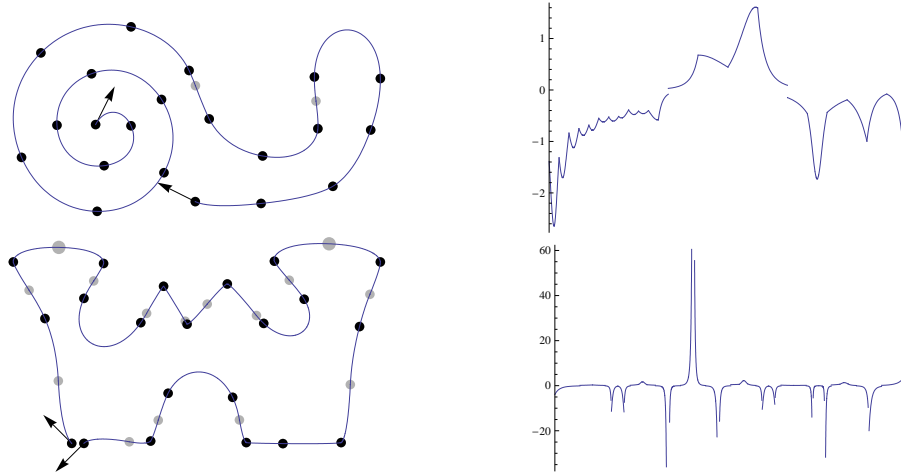

FIGURE 12. PH interpolating splines together with corresponding curvatures. Gray points are additional points determined by the preprocessing algorithm.
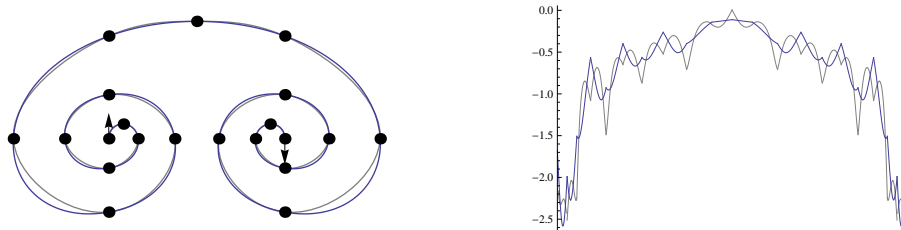

FIGURE 13. Cubic G^2 PH spline (black) and standard cubic C^2 spline (gray) together with the corresponding curvatures.

References

1. Gudrun Albrecht and Rida T. Farouki, *Construction of C^2 Pythagorean-hodograph interpolating splines by the homotopy method*, Adv. Comput. Math. **5** (1996), no. 4, 417–442. MR MR1414289 (97k:65033)
2. Carl de Boor, *A practical guide to splines*, revised ed., Applied Mathematical Sciences, vol. 27, Springer-Verlag, New York, 2001. MR MR1900298 (2003f:41001)
3. Rida T. Farouki, *The conformal map $z \to z^2$ of the hodograph plane*, Comput. Aided Geom. Design **11** (1994), no. 4, 363–390. MR MR1287495 (95f:65034)
4. ———, *Pythagorean-hodograph curves*, Handbook of computer aided geometric design, North-Holland, Amsterdam, 2002, pp. 405–427. MR MR1928550
5. ———, *Pythagorean-hodograph curves: algebra and geometry inseparable*, Geometry and Computing, vol. 1, Springer, Berlin, 2008. MR MR2365013 (2008k:65027)
6. Rida T. Farouki, Carla Manni, and Alessandra Sestini, *Shape-preserving interpolation by G^1 and G^2 PH quintic splines*, IMA J. Numer. Anal. **23** (2003), no. 2, 175–195. MR MR1974222 (2004c:65011)
7. Rida T. Farouki and C. Andrew Neff, *Hermite interpolation by Pythagorean hodograph quintics*, Math. Comp. **64** (1995), no. 212, 1589–1609. MR MR1308452 (95m:65025)
8. Rida T. Farouki and Takis Sakkalis, *Pythagorean hodographs*, IBM J. Res. Develop. **34** (1990), no. 5, 736–752. MR MR1084084 (92a:65063)
9. Yu Yu Feng and Jernej Kozak, *On G^2 continuous cubic spline interpolation*, BIT **37** (1997), no. 2, 312–332. MR MR1450963 (98c:65014)
10. Gašper Jaklič, Jernej Kozak, Marjeta Krajnc, Vito Vitrih, and Emil Žagar, *Geometric Lagrange interpolation by planar cubic Pythagorean-hodograph curves*, Comput. Aided Geom. Design **25** (2008), no. 9, 720–728. MR MR2468201
11. Bert Jüttler, *Hermite interpolation by Pythagorean hodograph curves of degree seven*, Math. Comp. **70** (2001), no. 235, 1089–1111 (electronic). MR MR1826577 (2002c:65027)
12. Dereck S. Meek and D. J. Walton, *Geometric Hermite interpolation with Tschirnhausen cubics*, J. Comput. Appl. Math. **81** (1997), no. 2, 299–309. MR MR1459031 (98b:65011)
13. ———, *Hermite interpolation with Tschirnhausen cubic spirals*, Comput. Aided Geom. Design **14** (1997), no. 7, 619–635. MR MR1467315 (98d:65020)
14. Francesca Pelosi, Maria Lucia Sampoli, Rida T. Farouki, and Carla Manni, *A control polygon scheme for design of planar C^2 PH quintic spline curves*, Comput. Aided Geom. Design **24** (2007), no. 1, 28–52. MR MR2286365
15. Zbyněk Šír and Bert Jüttler, *Euclidean and Minkowski Pythagorean hodograph curves over planar cubics*, Comput. Aided Geom. Design **22** (2005), no. 8, 753–770. MR MR2173576 (2006i:65021)

FMF, University of Ljubljana, and PINT, University of Primorska
Current address: Jadranska 19, 1000 Ljubljana, Slovenia
E-mail address: `gasper.jaklic@fmf.uni-lj.si`

FMF and IMFM, University of Ljubljana
Current address: Jadranska 19, 1000 Ljubljana, Slovenia
E-mail address: `jernej.kozak@fmf.uni-lj.si`

IMFM, University of Ljubljana
Current address: Jadranska 19, 1000 Ljubljana, Slovenia
E-mail address: `marjetka.krajnc@fmf.uni-lj.si`

PINT, University of Primorska
Current address: Muzejski trg 2, 6000 Koper, Slovenia
E-mail address: `vito.vitrih@upr.si`

FMF and IMFM, University of Ljubljana
Current address: Jadranska 19, 1000 Ljubljana, Slovenia
E-mail address: `emil.zagar@fmf.uni-lj.si`